A Liquid-Filled Buoyancy-Driven Convective Micromachined Accelerometer

Lin Lin and John Jones

Abstract—**A novel class of accelerometer, based on the buoyancy of a heated fluid within a micromachined cavity, has previously been developed and reported. Based on dimensional analysis and computational modeling, it is predicted that the sensitivity of the accelerometer can be increased by several orders of magnitude over previously reported results by choosing a suitable liquid as the working fluid, though this increased sensitivity comes at the cost of an increased response time. A liquid-filled accelerometer is constructed; its sensitivity and response time are measured, and shown to be consistent with theoretical predictions and with the results of finite-element analysis. It is noted that the existing literature provides no basis for predicting the effect of Prandtl number on the sensitivity and response time of the accelerometer. The prediction of response time requires analysis of the transient response of the heated fluid to a sudden acceleration. This is a novel problem: previous studies of transient convection have focused on the effects of a newly imposed temperature differential in an existing gravity field, rather than a newly imposed acceleration on an existing thermal field. An approximate expression for response time as a function of radius ratio and Prandtl number is developed by curve-fitting to the results of FLOTRAN simulation.   [1174]**

Index Terms—**Accelerometer, buoyancy, natural convection.**

I. INTRODUCTION

A NOVEL accelerometer design has recently been developed [1]. This design features a heater centrally placed within a fluid-filled cavity. The heater is maintained a constant temperature ΔT above the temperature of the wall of the enclosure, producing a radial temperature gradient. When an acceleration is applied, the heated fluid is displaced by buoyancy forces. The resulting temperature asymmetry, δT, is detected by temperature sensors symmetrically placed around the heating element and the acceleration deduced. This description can be realized in one of two forms: as a single-axis accelerometer, in which the heater and enclosure are concentric parallel cylinders or parallelopipeds; or as a multi-axis accelerometer, in which the heater and enclosure are concentric spheres or cuboids.

II. DIMENSIONAL ANALYSIS

We first perform a dimensional analysis to determine the parameters on which device performance will depend. In vector notation and using the Boussinesq approximation, the equations for the conservation of energy and momentum are, respectively, the following.

Energy:

$$\frac{\partial T}{\partial t} + (\mathbf{v}.\nabla)T = \alpha\nabla^2 T \tag{1}$$

where T represents local fluid temperature, $\mathbf{v}$ is a vector representing fluid velocity, and α is the thermal diffusivity of the fluid.

Momentum:

$$\frac{\partial \mathbf{v}}{\partial t} + (\mathbf{v}.\nabla)\mathbf{v} = \frac{-\nabla p}{\rho} + \frac{\mu}{\rho}\nabla^2\mathbf{v} - \beta(T - T_o)\nabla\mathbf{g} \tag{2}$$

where p is pressure, T_0 is the ambient temperature, and μ, ρ and β are the fluid viscosity, density and coefficient of thermal expansion, respectively.

Define τ as the time required for the temperature difference between the symmetrically placed temperature sensors to reach 63% of its steady-state value. We nondimensionalise these equations with respect to the reference quantities τ, T_o and r_i, the characteristic dimension of the heater.

Energy:

$$\frac{\partial \theta}{\partial \hat{t}} + (\hat{\mathbf{v}}.\hat{\nabla})\theta = F_o\hat{\nabla}^2\theta. \tag{3}$$

Momentum:

$$\frac{\partial \hat{\mathbf{v}}}{\partial \hat{t}} + (\hat{\mathbf{v}}.\hat{\nabla})\hat{\mathbf{v}} = -\hat{\nabla}\hat{p} + F_o P_r\hat{\nabla}^2\hat{\mathbf{v}} - F_o^2 P_r^2 G_r\hat{\nabla}\hat{\mathbf{g}} \tag{4}$$

where $\hat{\nabla}$ represents the derivative with respect to a nondimensional coordinate system, $\hat{\mathbf{g}}$ is a unit vector aligned with the gravitational field or imposed acceleration, and F_o is the Fourier number, $F_o = \tau\alpha/r_i^2$. (A more detailed derivation of the nondimensional form of the equations is given in [3].) It can be seen from these equations that for a given value of R, F_o depends only on the dimensionless groups R, G_r and P_r. The product $G_r P_r$ is often referred to as the Rayleigh number, R_a.

Previous papers on the thermal accelerometer [6] have noted the dependence of performance on Grashof number, but have not investigated the effect of Prandtl number on sensitivity or response time. There is thus no basis in the existing accelerometer literature for predicting the effect of a nongaseous working fluid on device performance. However, two papers on natural convection in enclosed fluids with a high degree of symmetry—concentric cylinders [11] and concentric spheres [12]—do provide some basis for prediction. Both [11] and [12] develop closed-form approximate solutions for the temperature field resulting from an acceleration, and both solutions yield an expression of

TABLE I
COMPARISON OF COMPUTED AND EXPERIMENTAL RESULTS

Working Fluid	Sensitivity to $1g$		Response Time	
	Air	Alcohol	Air	Alcohol
FLOTRAN	0.0031 K	2.17 K	6.3 ms	240 ms
Experiment	0.0036 K	2.54 K	25 ms	300 ms

the form $R_a f(R)\Delta T$ for the maximum temperature difference δT between diametrically opposed points, where $f(R)$ is a function of geometry depending only on the ratio R of the radii of inner and outer bounding surfaces. This expression implies that a liquid-filled accelerometer may be two or three orders of magnitude more sensitive than the air-filled accelerometer described in [1], and motivates the present work.

A. Validation of a FLOTRAN Model

Equations (1)–(4) were represented in the CFD package FLOTRAN. Accurate modeling of the accelerometer performance required exceptional care, as the quantity of interest, δT, is a small difference between two almost equal temperatures. Full details of the modeling process are provided in [3]. To validate the modeling method, the equations were first solved for two geometries for which closed-form solutions exist.

1) Concentric Cylinders Model: A pair of infinite concentric cylinders was modeled using the FLOTRAN program. To confirm that the model was correctly formulated, we compared its steady-state solution with that predicted by Hodnett [11]. The dimensionless differential temperature profile along the axis of acceleration predicted by the program was compared with the predictions of Hodnett's formula for the same case. Agreement was excellent—within 1% at all points.

2) Concentric Spheres Model: Next, a pair of concentric spheres was modeled using the FLOTRAN program, and its steady-state solutions for temperature and flow fields compared with Hardee's predictions in [12]. The mesh used for the spherical annulus was scaled to ensure that all elements were approximately cubic. Excellent agreement was obtained between the computed solution and the predictions of Hardee's formula.

3) Rectangular Parallelopiped Model: Lastly, a three-dimensional model of the chip used for experimental tests was constructed and run, using the same degree of mesh refinement as for the spherical model. Table I compares the predictions of the model with experimental results.

III. EXPERIMENTAL WORK

A. Construction of a Liquid-Filled Accelerometer

We were supplied with a number of accelerometer chips designed for use with air as a working fluid. A cross-section of one of these chips is shown in Fig. 1. The device consists of a cavity etched in silicon, spanned by a silicon bridge 20.6 microns wide and 3 microns deep, which is used as a heater. The cavity is 970 microns across in the direction parallel to the long axis of the heater, and 915 microns across in the orthogonal direction. Eight silicon bridges extend from each of the two side walls of the cavity to the edge of the heater The cross-section
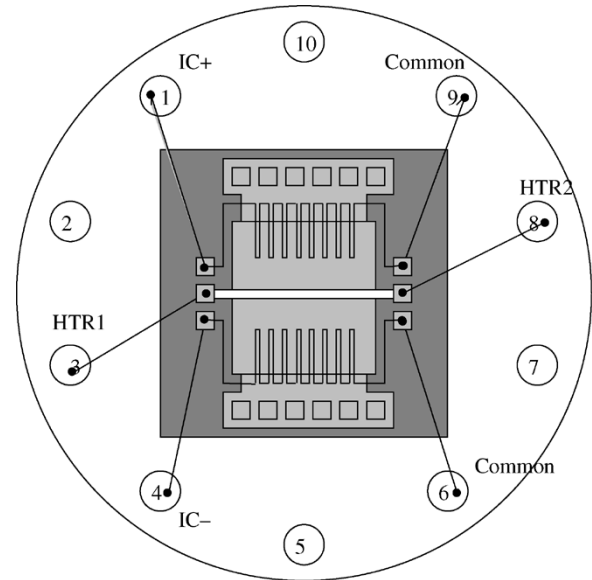
Fig. 1.   Cross-section of experimental chip.

of these bridges is approximately 3 μm by 20 μm. Each bridge carries a thermocouple at a distance of 300 microns from the cavity wall. The thermocouples are an integral part of the chip, and consist of aluminum films deposited on silicon, having a sensitivity of approximately 100 μV/K. The chip is designed to measure accelerations acting in the plane containing the heater and thermocouples, orthogonal to the heater.

The depth of the etched cavity below the plane of the heater and detectors was 230 microns. The chip was packaged in a TO-100 metal can package, leaving the cavity unsealed above the heater plane, but covered by a metal cap giving about 1000 microns clearance above the heater plane.

B. Temperature Profile of Heater

To allow us to determine the temperature at the heater during operation, we placed the chip in an environmental chamber and heated it by stages from 20 °C to 120 °C, measuring the resistance of the heater at each stage. The resistance was found to increase as a linear function of temperature. In using this correlation to interpret experimental measurements, we note that in operation, though not in the environmental chamber, the heater loses heat by axial conduction to the cavity walls. This results in a nonuniform temperature profile, which can be calculated as follows:

Consider one-half of the heater as a prism having cross-sectional area A, cross-sectional perimeter P and length L, surrounded by air at a uniform temperature. One end of the heater is fixed at the wall temperature, which is the same as the air temperature, T_0. The other end, corresponding to the mid-point of the heater, has the boundary condition $dT/dx = 0$, from symmetry. Heat is generated within the heater at a rate $q\,\text{W/m}^3$. The temperature distribution in the heater, $T(x)$, can be represented by the differential equation

$$\frac{d^2T}{dx^2} - \frac{hP}{kA}(T(x) - T_0) + \frac{q}{k} = 0 \qquad (5)$$
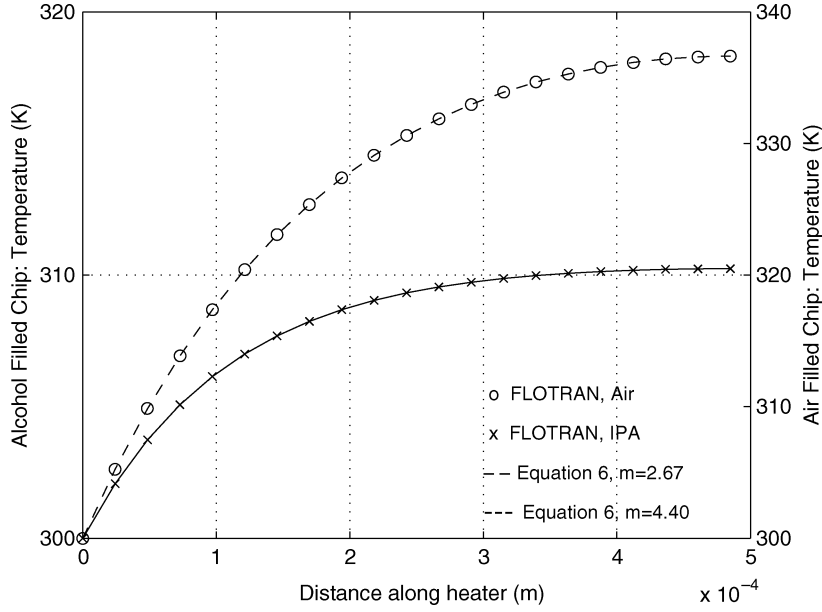
Fig. 2. Analytic and numerical solutions for heater temperature profile.

where h is the convective heat transfer coefficient and k is the conductivity of the heater material. This can be solved to give

$$T(x) - T_0 = \frac{qL^2}{km^2}\left(1 - e^{\frac{mx}{L}} + e^m\frac{\sinh\left(\frac{mx}{L}\right)}{\cosh(m)}\right) \quad (6)$$

where $m^2 = hPL^2/kA$. Note that the shape of the temperature profile depends only on m, not on q.

Fig. 2 compares the profiles predicted by (6) with the profiles calculated by FLOTRAN for chips with working fluids of air and isopropanol. The profiles calculated from (6) are shown as dashed and solid lines, respectively, while the datapoints taken from the FLOTRAN simulation are shown as circles and crosses, again respectively. This fit was obtained by setting the value of h in (6) to 1600 W/m.K for air, yielding $m = 2.67$, and to 4300 W/m.K for isopropanol, corresponding to $m = 4.4$. The higher value of h for isopropanol is due to its higher thermal conductivity. (We note that, as shown by Hodnett in [11], the heat loss from the heater to the fluid is almost entirely due to thermal conduction rather than convection.)

If the heater is measured to have a resistance corresponding to a uniform temperature of T_1, the actual heater temperature will have the profile shown, where the maximum value T_2 is given by

$$\frac{T_2 - T_0}{T_1 - T_0} = \frac{L}{\int_0^L\left(1 - e^{\frac{mx}{L}} + e^m\frac{\sinh\left(\frac{mx}{L}\right)}{\cosh(m)}\right)dx}. \quad (7)$$

This gives a correction factor of $T_2 - T_0 = 1.59(T_1 - T_0)$ for air and $(T_2 - T_0) = 1.29(T_1 - T_0)$ for isopropanol.

C. Response Time of Detectors

The FLOTRAN model calculates the time taken for the temperature at a given radial location to reach 63% of its final value. The actual response time of the accelerometer will exceed this

by the time taken for the thermocouples to register that change in temperature.

The characteristic response time for a thermocouple is

$$\tau_c = \frac{\rho V c_p}{hA} \quad (8)$$

where ρ is the density of the thermocouple material, V its volume, c_p its specific heat, A its area, and h the convective heat transfer coefficient. From (6), and using the values of h calculated in the previous section, τ_c for the thermocouples used in the air-filled chip is of the order of 2 ms, falling to about 0.75 ms for the alcohol-filled chip. For comparison, FLOTRAN calculated the time for the temperature differential to develop in the working fluid to be about 4 ms for the air-filled chip, and about 300 ms for the alcohol-filled chip.

D. Steady-State Response

A voltage of 5 V was put across the heater of the air-filled chip, resulting in a maximum temperature difference $T_2 - T_0$ of 60 K. A Wheatstone bridge circuit was used to measure the difference in temperature between the thermocouples to either side of the heater bridge, and the resistances in the circuit adjusted so that the differential signal was zero when no acceleration was applied. The chip was then tilted through ninety degrees, giving a 1-g acceleration. The measured differential signal, summed over the eight pairs of thermocouples, was of the order of 10 microvolts, corresponding to a value of δT for each pair of thermocouples of about 0.012 K. We constructed an amplifier circuit, using an AD 620 and AD 625 amplifier chip, to increase the summed response by a factor of about 1000.

1) Liquid-Filled Chip: Linearity and Saturation: After removing the chip's metal cap, we found it relatively straightforward to fill the chip cavity with isopropanol, using a fine syringe. Microscopic inspection of the chip did not detect any bubbles of trapped air. The cap was separately filled with isopropanol. We
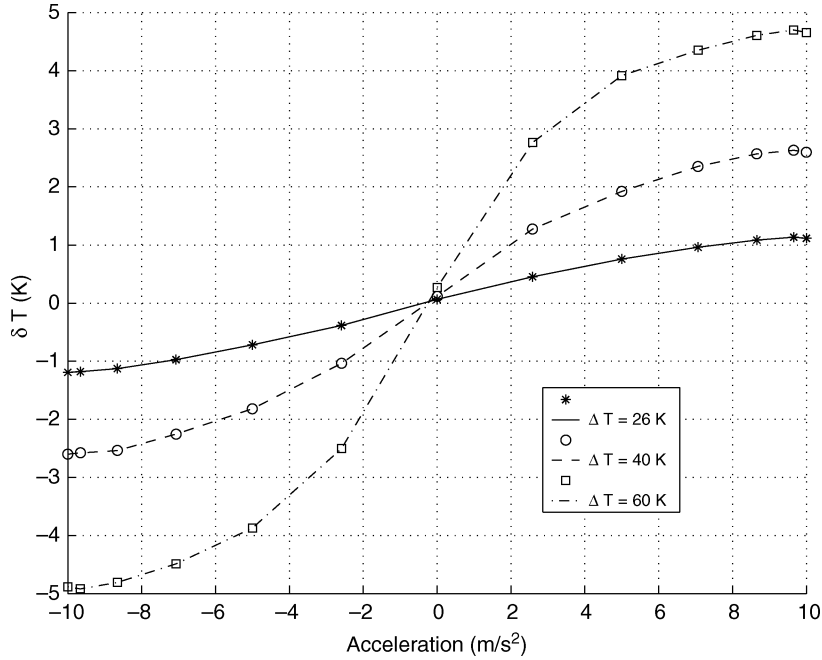
Fig. 3. Response with increasing acceleration.

then inverted the chip and lowered it onto the isopropanol-filled cap. The surface tension of the liquid was sufficient to keep the cavity full of isopropanol during this operation. While not vapor-proof, this arrangement was found adequate to keep the chip charged with isopropanol for about 24 h. We took the isopropanol-filled chip and increased the voltage across the heater by stages, from 3 V to 6 V. The heater temperature was estimated at each stage by measuring its electrical resistance and applying the correction factor derived in (7). Ambient temperature was 300 K. The linearity of the accelerometer response was assessed at each voltage level by gradually tilting the accelerometer from the horizontal to a vertical plane, with results shown in Fig. 3.

It may be seen that the response is initially linear, becoming sub-linear before reaching $1g$. The higher the value of ΔT, the difference between ambient temperature and heater temperature, the lower the value of acceleration at which the response becomes sublinear. This may be due to device saturation: the value of R_a at which the measured response falls below linearity is of the same order of magnitude as the linearity limit calculated in [11], and the reduction of the threshold value of acceleration with increasing ΔT is consistent with the dependence of R_a on ΔT. However, it is also possible that the fall-off in performance results from the vaporization of the alcohol, which has a boiling point of 80 $^\circ$C, adjacent to the hottest part of the heater.

2) Comparison With Air-Filled Chip: The response of the isopropanol chip to a $1-g$ acceleration at a series of heater temperatures was then compared with the response of an identical air-filled chip for the same values of ΔT. From the results given in [11] and [12] for cylindrical and spherical geometries, and from FLOTRAN simulations of the experimental geometry, we expect the sensitivity of the chip to be proportional to $R_a \Delta T$.

R_a itself contains an additional factor of ΔT, so in Fig. 4 we plot the sensitivities of the two chips against $(\Delta T)^2$.

From the dependence of R_a on the properties of the working fluid, we deduce that the sensitivities of the air and alcohol-filled chips should be in the ratio

$$\frac{\delta T_i}{\delta T_a} = \frac{\rho_i^2 \beta_i c_{pi} k_a \mu_a}{\rho_a^2 \beta_a c_{pa} k_i \mu_i} = \frac{790^2 \times 62 \times 2440 \times 26 \times 2}{1^2 \times 330 \times 1000 \times 119 \times 177} = 700 \tag{9}$$

where the subscripts a and i denote the properties of air and isopropanol, respectively.

Both plots are initially linear, and, over this range, the sensitivity of the alcohol-filled chip is approximately 700 times that of the air-filled chip. Beyond the initial, linear region of the graph, the response of the alcohol-filled chip falls off. Note that the power required to maintain a particular value of ΔT is greater for the liquid-filled chip, due to the higher thermal conductivity of the liquid. Thus a comparison of the two chips on the basis of equal power supplied to the heater would show a smaller, though still significant, advantage to the liquid-filled variant.

E. Transient Response

To measure the transient response of the chip, it was mounted on a Brüel and Kjær PM Vibration Exciter Type 4808 and subjected to a sinusoidally varying acceleration at a frequency gradually increasing from 1 Hz to 1 kHz. For both air-filled and isopropanol-filled chips, the chip output signal followed the imposed acceleration, but its amplitude fell off after a certain point.

During these measurements, care had to be taken to ensure that the amplifier circuitry was not picking up an electrical signal generated by the vibration table itself. This was achieved
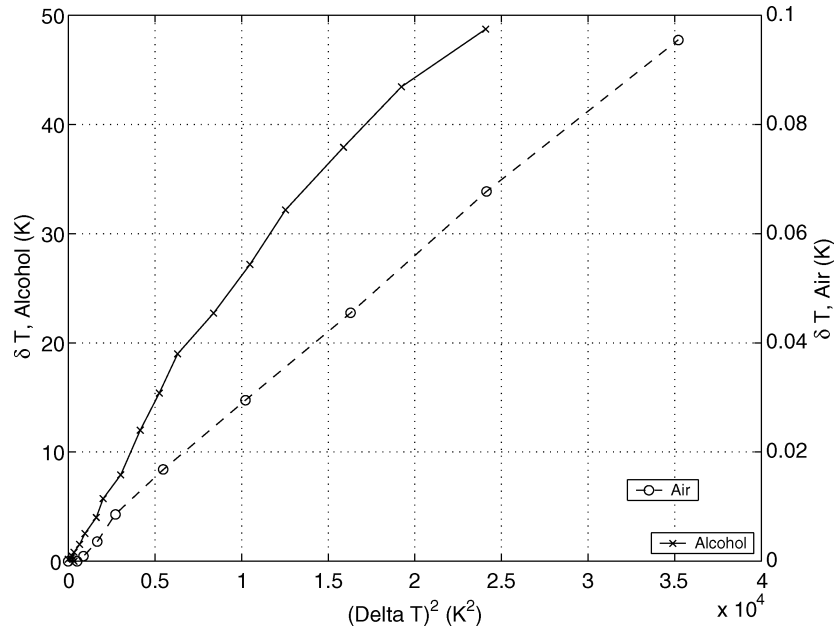
Fig. 4.   Temperature difference as a function of heater temperature.
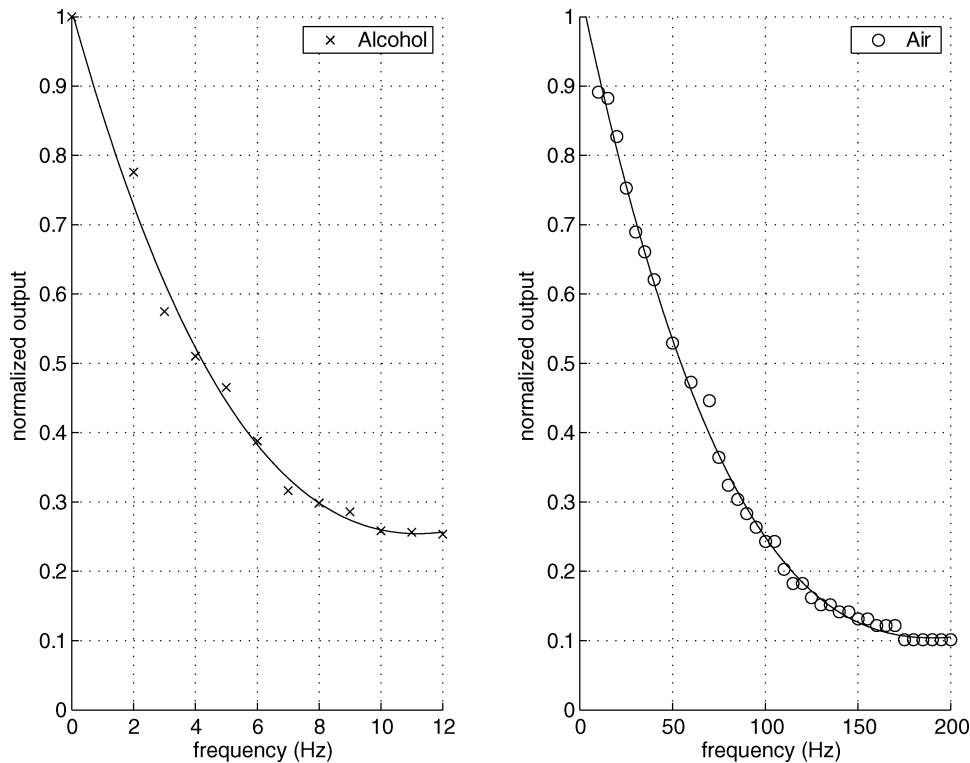
Fig. 5.   Decay of signal with increasing frequency.

by very careful shielding of the circuits. We confirmed that the signal measured was indeed generated by the differential temperatures at the detectors by switching off the power to the heater at intervals during the experiment: the output signal then quickly faded, confirming that we were measuring accelerometer output rather than electrical noise. Fig. 5 shows the amplitude of the response as a function of frequency for

both working fluids. In each case, a cubic polynomial has been interpolated to the datapoints.

Table I compares the predictions of the model with experimental results. The comparison is made on the basis of $T_2 - T_0 = 37$ K. The thermocouple response time calculated from (8) has been added to the response time predicted by FLOTRAN.

The most salient discrepancy between model and experiment is in the response time of the air-filled accelerometer. In addition, with increasing frequency the response of each chip appears to fall, not to zero, but to a value of 10–25% of the steady-state response. The reason for this is not fully understood.

IV. DESIGN GUIDELINES FOR CHOICE OF WORKING FLUID

As noted, no prior work has discussed the possibility of using a liquid as the working fluid for a convective accelerometer, or developed a basis for predicting the sensitivity or response time for such a design. In this section, we identify published results that can provide an approximate value for device sensitivity, and conduct a series of FLOTRAN simulations that permit approximate prediction of the effect of working-fluid Prandtl number on response time.

A. Cylindrical and Spherical Approximations

As noted, closed-form approximate expressions have been developed for the temperature field created by natural convection in two idealised geometries, concentric cylinders and concentric spheres [11], [12], both having the form

$$\delta T = R_a f(R) \Delta T \qquad (10)$$

To evaluate a proposed design, we may select one or other of these geometries—the spherical geometry is a better approximation to a two-axis accelerometer, while the cylindrical geometry approximates a single-axis design—define inner and outer radii based on the device dimensions, and evaluate this expression. The absolute values of sensitivity so calculated are only a fair approximation to measured performance, underestimating sensitivity by a factor of two. However, once a single datapoint has been obtained by simulation or experiment, (10) may then be used to predict the relative sensitivity of the device for other working fluids or other choices of ΔT.

B. Factors Affecting Device Response Time

In addition to the magnitude of the response to acceleration, we are also concerned with the time taken for this response to develop. We again suppose that the response time of the device can be estimated by solutions for the cylindrical and spherical geometries. However, this problem differs from the transient cases discussed in the prior literature, both for the cylindrical case ([13]–[16]) and the spherical case ([13], [17], [18]), in that the transient develops due to the suddenly imposed acceleration rather than the heating of one bounding surface. We have therefore undertaken a series of FLOTRAN studies to establish correlations for response time.

Possible working fluids for the accelerometer fall into three classes: low-Prandtl-number fluids, such as mercury; intermediate-Prandtl-number fluids, including air and other gases; and high-Prandtl-number fluids, such as oil. In each case, when the acceleration is applied, the pre-existing symmetric temperature field creates a buoyancy force, as a result of which a velocity field develops. This velocity field then creates an asymmetry in the temperature field. FLOTRAN simulation shows that for low-Prandtl-number fluids, the time taken for the velocity field

TABLE II
CORRELATIONS FOR FOURIER NUMBER FOR CYLINDRICAL GEOMETRIES

Prandtl No.	Correlation
Low	$F_o P_r / R^2 = \exp(-3.7166 - 2.6182/R + 0.0258 \ln R)$
$P_r = 0.7$	$F_o / R^2 = \exp(-1.9133 - 2.6977/R - 0.1 \ln R)$
High	$F_o / R^2 = \exp(-2.2345 - 2.4101/R - 0.1851 \ln R)$

TABLE III
CORRELATIONS FOR FOURIER NUMBER FOR SPHERICAL GEOMETRIES

Prandtl No.	Correlation
Low	$F_o P_r / R^2 = \exp(-3.1824 - 3.5873/R - 0.1998 \ln R)$
$P_r = 0.7$	$F_o / R^2 = \exp(-0.9853 - 3.8075/R - 0.6124 \ln R)$
High	$F_o / R^2 = \exp(0.1061 - 5.5416/R - 1.3999 \ln R)$

TABLE IV
FLUID PROPERTIES

Fluid	ρ	c_p	k	μ	Pr
	kg/m^3	J/kg.K	W/m.K	Pa.s	—-
Air	1.1768	1004	0.026	0.000018	0.7153
Isopropanol	932	2440	0.119	0.00177	36.3
Glycerine	1260	2400	0.286	1.5	12587
Mercury	13595	139	8.141	0.0017	0.029

TABLE V
EFFECT OF PRANDTL NUMBER ON RESPONSE TIME

Fluid	τ (cyl)	$\tau (sph)$	τ (FLOT.)
	ms	ms	ms
Air	1.6	0.73	4.3
Isopropanol	263	38	240
Glycerine	200	32	80
Mercury	100	75	90

to develop is much greater than the time for the resulting temperature differential to develop. For these cases, F_o is a function of both R and P_r. For high-Prandtl-number fluids, the velocity field develops relatively quickly, and it is the subsequent development of the temperature differential that determines the response time; in these cases, F_o depends only on R. For intermediate values of Prandtl number, the two processes overlap, and the correlation between F_o and R must be found separately for each particular value of P_r. These correlations have been found by curve-fitting to the results of numerous FLOTRAN simulations, and are given in Table II and III.

These correlations were used to derive upper and lower bounds on device sensitivity and response time for fluids having a range of Prandtl numbers. Table IV summarizes the physical properties of those fluids, while Table V compares their bounds with the results of FLOTRAN simulation of the experimental chip. (It is acknowledged that constructing a chip having mercury as the working fluid may present practical problems: it is included here to show the applicability of this approach to low-Prandtl-number fluids.)

It may be seen that the cylindrical and spherical solutions provide upper and lower bounds, respectively, on the response time calculated for the chip by FLOTRAN.

C. Device Saturation

As the Rayleigh number in an accelerometer is increased, the device will eventually saturate, that is, the temperature dif-
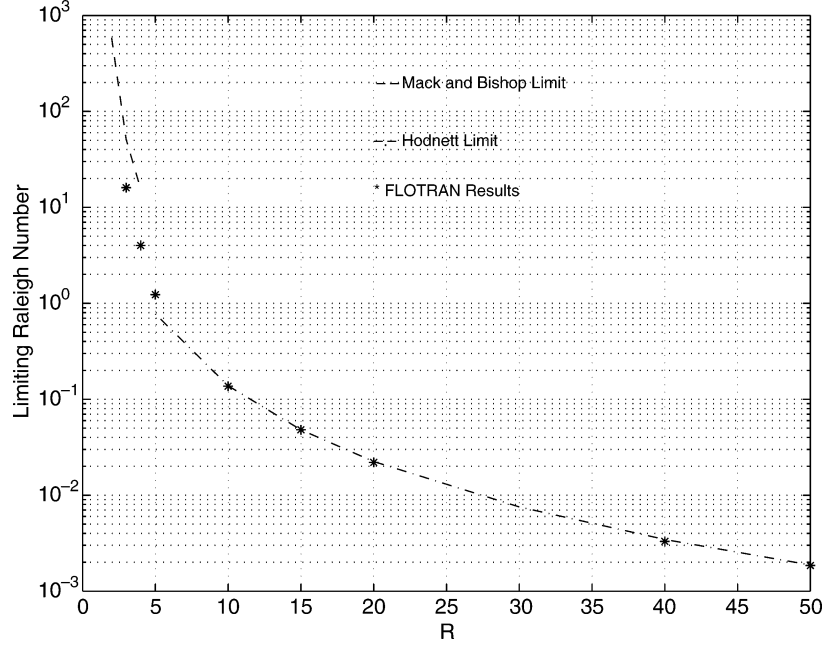
Fig. 6. Linearity limit on R_a as a function of R.

ferential between the detectors will no longer increase linearly with R_a. This effect may be seen in [1], Fig. 8, as the Rayleigh number is increased by pressurization of the working gas.

For cylindrical geometries Hodnett, in [11], shows that the upper bound of Rayleigh number for which the linear dependence of δT on R_a remains valid scales as $R^3/\ln R$ for large values of R. For lower values, he quotes the upper bound derived by Mack and Bishop in [9]. To confirm this, we conducted a series of FLOTRAN simulations at various values of R, recording the value of R_a at which the discrepancy between the numerical solution and the value of δT first exceeded 5%. These values are compared with Mack and Bishop's limit and the expression 60 $R^3/\ln R$ in Fig. 6, showing good agreement across a range of values.

For the spherical case, Fendell, [19], shows that the limiting value of R_a scales as $1/R^2$.

D. Lower Bound on Size

Given the current rate of progress in the MEMS field, it is difficult to set a lower limit on the size of accelerometer that can be constructed. However, a hard lower bound is set by the kinetics of the working gas: if the temperature of the gas is measured with a sufficiently small detector over a short time interval, a relatively small number of gas molecules will come into contact with the detector, and the mean kinetic energy of this small sample may differ from the mean kinetic energy of the gas as a whole. This will introduce noise into the measurements, and the noise will be greater as the size of the detector decreases.

If we represent the velocity of a gas molecule selected at random by

$$v = v_m + \Delta V \tag{11}$$

where v_m is the root-mean-square (rms) velocity of the gas molecules, and ΔV is the difference between the mean velocity

and the velocity of the selected molecule. it can be shown that the mean value of $(\Delta V)^2$ is given by

$$\Delta V^2 = \frac{kT\left(3 - \frac{8}{\pi}\right)}{m}. \tag{12}$$

From this we can calculate the mean temperature fluctuations of a system made up of a single molecule.

By the Central Limit Theorem, the mean temperature fluctuations of an ensemble of N molecules scale as $1/\sqrt{N}$. The temperature fluctuations measured by the thermometer are of size

$$\Delta T_t = \frac{\Delta T_g c_{pg} m_g}{c_{pt} m_t + c_{pg} m_g} \tag{13}$$

where c_p is specific heat, m is mass, and the subscripts t and g denote the detector and the gas ensemble, respectively. Equation (12) attains its maximum value when the thermal mass of the gas ensemble we are considering is comparable with that of the detector.

A cylindrical detector made of silicon, radius 0.1 μm, length 500 μm, has a thermal mass of about 10^{-10} J/K. This corresponds to an ensemble of 2×10^{12} air molecules. The fluctuations measured by the detector will therefore be about 10^{-6} times smaller than the temperature fluctuations of a single air molecule, that is, 0.1 mKelvin or smaller. For comparison, the temperature differential between the detectors of the accelerometer described in the following section is about 0.1 K for a 1-g acceleration when the working fluid is air, and about 10 K for a liquid (isopropanol).

E. Other Considerations

In addition to the factors discussed above, there will be some practical limitations on choice of working fluid. Isopropanol has a relatively low surface tension, which facilitated the filling of the chip cavity without entrapment of air bubbles; this might

TABLE VI
COMPARISON OF CAPACITIVE AND CONVECTIVE ACCELEROMETERS

Type	Capacitive	Convective (Air)	Convective (IPA)
Sensitivity	20 mV/g	100mV/g	7V/g
Bandwidth	1 kHz	160 Hz	5 Hz
Range	$\pm$ 2 g to $\pm$ 50 g	$\pm$ 1 g to $\pm$ 100 g	$\pm$ 1 mg to $\pm$ 1 g
Max. Accel.	1450 g	50,000 g [2]	50,000 g[a]

[a]Conjectured

be a greater problem with more viscous fluids. The use of an electrically conductive fluid would also present difficulties.

V. COMPARISON WITH PRIOR WORK

A. Comparison With Other Micromachined Accelerometers

A variety of micromachined accelerometers exist. One of the most popular is the interlocking-comb electrostatic accelerometer [8]. Table VI compares the performance of a representative example of this type, the Analog Devices ADXL50, with liquid-filled and air-filled variants of the current design. The maximum acceleration survivable by the liquid-filled chip has not been directly tested, but we conjecture that it will be no less than that of the air-filled design.

The capacitive accelerometer senses an acceleration by the deflection of a set of beams. Larger accelerations will cause larger deflections, and eventually failure. There is thus a trade-off between device sensitivity and device robustness. Because it lacks a solid proof mass, the convective accelerometer does not face this trade-off. Thus, it is well-suited to applications in which the instrument must measure small accelerations, while surviving high accelerations, for example, the accelerations of spacecraft launch or re-entry.

The most salient weakness of the thermal convective accelerometer is its slow response time, and this is exacerbated when we consider a liquid as the working fluid. However, the design relationships derived in the previous section suggest a possible solution to this problem: it has been shown that the isopropanol-filled chip is approximately 1000 times as sensitive as the air-filled chip, but also approximately 40 times slower to respond to an acceleration. If we reduce r_i and r_o for this chip by a factor of 10, the Rayleigh number will be reduced by a factor of 1000, as will the differential temperature signal. The response time of the shrunken isopropanol chip will be reduced by 100 times as a result of the shrinkage, which will make it more than twice as fast than the air-filled chip.

So we can trade off increased sensitivity against response time to get an isopropanol-filled chip that is as sensitive, at least as fast, and ten times smaller than an air-filled chip. It is possible that a systematic survey of potential working fluids would identify other options with further improvements in performance.

B. Prior Work on Thermal Convective Accelerometers

In addition to the design discussed in this paper, the device described in [4], in which the motion of a hot, solid proof mass is detected by its approach to a thermocouple, has also been described as a thermal convective accelerometer. Since it relies on a proof mass, however, it does not have the simplicity and robustness of the fluid-based convective accelerometer.

VI. CONCLUSION

On the basis of published expressions for convection in enclosed fluids, we have conjectured that it is possible to construct liquid-filled micromachined accelerometers having sensitivities up to three orders of magnitude greater than previously reported. FLOTRAN modeling supports this conclusion, and suggests that the response time of the liquid-filled accelerometer will be increased by about a factor of 40. An isopropanol-filled accelerometer has been constructed. Its sensitivity has been found to be about seven hundred times that of the same chip filled with air, in line with prediction. Its response time is at least an order of magnitude greater than that of the air-filled chip, though not two orders of magnitude greater, as theory would imply. A residual response to high-frequency acceleration is seen, the reasons for which are not understood.

Equations have been given that can be used to predict the effects of working-fluid properties and heater temperature on device sensitivity and response time. Upper and lower bounds on device size have been established. The liquid-filled accelerometer has been compared with other micromachined accelerometers: its strength is its combination of high sensitivity with great robustness, while its chief weakness is its slow response time.

REFERENCES

[1] A. Leung, J. Jones, E. Czyzewska, J. Chen, and M. Pascal, "A micromachined accelerometer with no proof mass," in *Technical Digest of Int. Electron. Device Meeting (IEDM97)*, Washington, DC, Dec. 1997, pp. 899–902.

[2] R. Dao, "Mechanical Shock Test Report: Accelerometer Model MXR7202ML,", Nov. 2003.

[3] L. Lin, "Design and Analysis of Microthermal Accelerometer," PhD Thesis, Simon Fraser University, Burnaby, Canada, Mar. 2004.

[4] R. Hiratsuka, D. C. van Duyn, T. Otaredian, and P. de Vries, "Design considerations for the thermal accelerometer," *Sens. Actuators A, Phys.*, vol. 32, pp. 380–385, 1992.

[5] V. Milanovic, E. Bowen, M. Zaghoul, N. Tea, J. Suehle, B. Payne, and M. Gaitan, "Micromachined convective accelerometers in standard integrated circuits technology," *Appl. Phys. Lett.*, vol. 76, no. 4, pp. 508–510, 2000.

[6] X. Luo, Y. Yang, F. Zheng, Z. Li, and Z. Guo, "An optimized micromachined convective accelerometer with no proof mass," *J. Micromech. Microeng.*, vol. 11, pp. 504–508, 2001.

[7] T. Kuehn and R. Goldstein, "An experimental and theoretical study of natural convection in the annulus between horizontal concentric cylinders," *J. Fluid Mech.*, vol. 74, no. 4, pp. 695–719, 1976.

[8] W. Kuehnel and S. Sherman, "A surface micromachined silicon accelerometer with on-chip detection circuitry," *Sens. Actuators A, Phys.*, vol. 45, pp. 7–16, 1994.

[9] R. Mack and E. Bishop, "Natural convection in the space between horizontal concentric cylinders for low Rayleigh numbers," *Quart. J. Mech. Appl. Math.*, vol. 21, pp. 223–241, 1968.

[10] Z. Rotem, "Conjugate free convection from horizontal conducting circular cylinders," *Int. J. Heat Mass Transfer*, vol. 15, pp. 1679–1693, 1972.

[11] P. Hodnett, "Natural convection between horizontal heated concentric circular cylinders," *J. Appl. Math. Phys.*, vol. 24, pp. 507–516, Nov. 1973.

[12] H. Hardee, "Natural convection between concentric spheres at low Rayleigh numbers," Ph.D. dissertation, University of Texas, Austin, May 1966.

[13] K. Kübleck, G. Merker, and J. Straub, "Advanced numerical computation of two-dimensional time-dependent free convection in cavities," *Int. J. Heat Mass Transfer*, vol. 23, pp. 203–217, 1980.

[14] Y. Tsui and B. Tremblay, "On transient natural convection heat transfer in the annulus between concentric horizontal cylinders with isothermal surfaces," *Int. J. Heat Mass Transfer*, vol. 27, no. 1, pp. 103–111, 1984.

[15] A. Castrejon and D. Spalding, "An experimental and theoretical study of transient free-convection flow between horizontal concentric cylinders," *Int. J. Heat Mass Transfer*, vol. 31, no. 2, pp. 273–284, 1988.

[16] K. Vafai and J. Ettefagh, "An investigation of transient three-dimensional buoyancy-driven flow and heat transfer in an closed horizontal annulus," *Int. J. Heat Mass Transfer*, vol. 34, no. 10, pp. 2555–2570, 1990.

[17] L. Mack and H. Hardee, "Natural convection between concentric spheres at low Rayleigh numbers," *Int. J. Heat Mass Transfer*, vol. 11, pp. 387–396, 1968.

[18] J. P. Caltagirone, M. Combarnous, and A. Mojtabi, "Natural convection between two concentric spheres: transition toward a multicellular flow," *Num. Heat Transfer*, vol. 3, pp. 107–114, 1980.

[19] F. Fendell, "Laminar natural convection about an isothermally heated sphere at small Grashof number," *J. Fluid Mech.*, vol. 34, pp. 163–176, 1968.

Lin Lin received the B.A.Sc. degree in electrical engineering from Xidian University, Xi An, China, in 1990. She then worked as a computer programmer in a telecommunications company in South China for two years. She joined the M.A.Sc. program in the School of Engineering Science at Simon Fraser University (SFU) in 1995 after immigrating to Canada. Her M.A.Sc. research project involved numerical modeling of pressure-swing adsorption, a chemical/physical process used for hydrogen purification and oxygen/nitrogen separation. She worked as a modeling engineer in the affiliated industrial company for one year, then returned to SFU to pursue the Ph.D. degree with research on the design and analysis of the microthermal accelerometer, which included theoretical investigation, numerical simulation, and experimental study. This work is summarized in the present paper and is presented in greater detail in her dissertation, published in March 2004.

Her current research interests include the theoretical study and numerical modeling of heat transfer and fluid flow in micromachined/microfluidic devices.

John Jones received the B.Sc. degree in mathematical physics from the University of Sussex, U.K., in 1974. After several years as a schoolteacher in rural Kenya, he received the Ph.D. degree in engineering at the University of Reading, U.K., and then worked as an engine designer for General Motors Research Laboratories.

He joined Simon Fraser University, Canada, in 1988 and has worked there since. His current research interests include heat transfer, Stirling engines, and the application of artificial intelligence to engineering design.